12th Brazilian Congress of Manufacturing Engineering
May 10th-12th, 2023, Brasilia, DF, Brazil

PHOTOGRAMMETRY APPLIED FOR INSPECTION OF ADDITIVE MANUFACTURED COMPONENTS

Daniel de Moraes Coelho
Federal University of Uberlândia, School of Mechanical Engineering, Center for Research and Development of Welding Processes, Uberlândia, Minas Gerais, Brazil
danielcoelho@ufu.br

Luiz Eduardo dos Santos Paes
Federal University of Uberlândia, School of Mechanical Engineering, Center for Research and Development of Welding Processes, Uberlândia, Minas Gerais, Brazil
luiz.paes@ufu.br

Alexandre Zuquete Guarato
Federal University of Uberlândia, School of Mechanical Engineering, Center for Research and Development of Welding Processes, Uberlândia, Minas Gerais, Brazil
azguarato2@gmail.com

Douglas Bezerra de Araújo
Federal University of Uberlândia, School of Mechanical Engineering, Center for Research and Development of Welding Processes, Uberlândia, Minas Gerais, Brazil
dbaraujo@ufu.br

Fernando Matos Scotti
Federal University of Uberlândia, School of Mechanical Engineering, Center for Research and Development of Welding Processes, Uberlândia, Minas Gerais, Brazil
fernandomscotti@gmail.com

Louriel Oliveira Vilarinho
Federal University of Uberlândia, School of Mechanical Engineering, Center for Research and Development of Welding Processes, Uberlândia, Minas Gerais, Brazil
vilarinho@ufu.br

Abstract. *Three-D scanning methods can be used to reconstruct a part for different industrial purposes, varying from reverse engineering to dimensional inspection of a gas turbine. A wide variety of scanners is available, classified as active or passive sensors. In active sensors, as in laser scanning, energy is transmitted to the scene and the reflected energy is recorded. In contrast, passive sensors do not transmit energy but use natural light available to acquire information. An example of a technique that uses this last type of sensor is photogrammetry. Photogrammetry is an optical measurement technique that is used to obtain the geometry, displacement, and deformation of a structure using photographs. This technique can be used in several fields, such as medicine, biological sciences, civil construction, archeology and general inspection. Additive manufactured components require a strict inspection process before going into service, which demands qualified professionals, incurring into extra expenses to attest their integrity. Since the first stage of the process is visual inspection, this study presents the application of photogrammetry technic to inspect Wire Arc Additive Manufactured (WAAM) components. A 3D model is generated using a commercial DSLR camera combined with an open-source software, and it is compared with another one generated with a commercial laser scanning system. The accuracy of the photogrammetry system was 0.144 mm, from which 0.104 mm was due to the average measurement deviation between the models and 0.040 mm from the inner accuracy of the laser scanning system, making it adequate to inspect a 115 mm diameter component. The photogrammetry model was the only one that had color representation and, since small discontinuities that do not present large geometrical variations can be identified through the surface colors, this is fundamental for visual inspection. This study should also serve as stimulus for other researchers and engineers to use remote visual inspection through 3D models and virtual reality (VR).*

Keywords: *3D scanning; Non-Destructive-Tests (NDT); Directed Energy Deposition; Welding; Virtual Reality;*

1. INTRODUCTION

The presence of additively manufactured (AM) metallic components has increased in different industrial sectors. Design freedom aiming at optimizing material strength for minimum weight (Hodonu *et al.*, 2019), manufacturing of

functionally graded materials (Li *et al.*, 2020) and personalization of prosthesis (Sohaib *et al.*, 2018, Dos Santos *et al.*, 2019) can be cited among its benefits. In addition, this is a sustainable approach, since material loss is much lower than that observed in other processes, such as machining.

Among the applications in which additive manufacturing stands out, is the production of spare parts. Many companies need to keep inventories, significantly increasing costs (Bacciaglia *et al.*, 2020). This technology allows building virtual libraries and manufacture parts on demand. However, some sectors, such as oil and gas, require strict certification processes, which may imply in reposition delays. Chua *et al.* (2017) state that one of the main barriers for the adoption of additive manufacturing is related to qualification. Quality control is still a challenge and hinders the diffusion of AM.

The process of directed energy deposition (DED) with electric arc and wire feeding, known as Wire Arc Additive Manufacturing (WAAM), is preferred for medium to large size components. It is possible to reach high deposition rates with a MIG/MAG torch, which contributes for the reduction of manufacturing time. Other arc processes, such as TIG, can also be used (Bai *et al.*, 2016), but its advantages and modern variants as the wire oscillating (Silva *et al.*, 2019a, Silva *et al.*, 2019b) have not been explored yet. DED with laser is another trend, focused on reduced size components (Paes *et al.*, 2021). Laser energy concentration allows reaching high resolution, although it should be controlled in order to prevent possible defects (Paes *et al.*, 2019a, Paes *et al.*, 2019b, Neto *et al.*, 2021). Figure 1 shows the first additive manufactured part applied in an oil and gas facility in Brazil (Petrobras, 2019).

Figure 1. The first additive manufactured (WAAM) part applied in an oil and gas facility in Brazil.

This part is a carbon steel tube transition (sleeve), initially produced of cast iron by using conventional manufacturing processes. Mechanical and non-destructive tests demonstrated its integrity and the first stage of qualification regards visual inspection. The component surface presents a characteristic waviness, which has to be homogeneous to allow further machining. Arc instability issues can lead to the lack of homogeneity in deposition (Silva *et al.*, 2018, Truppel *et al.*, 2019, Sartori *et al.*, 2017). The mentioned test is also used to detect external defects.

Visual inspection must be performed by certified professionals. Particularly, for WAAM, professionals with MIG/MAG welding experience are required. A fundamental constraint is in situ inspection (the inspector must visit the facility), incurring in traveling expenses. In addition, inspectors usually use welding gauge kits with reduced accuracy, and that do not allow digital recording for future evaluations. Another issue is related to inspector training. Defects must be induced purposefully in components. According to Martín and Gonzalvez (2018), for welding inspection, each part costs between $ 200 and $ 3,000. Costs are even greater for additively manufactured parts. Also, building a complete learning laboratory is laborious and expensive. In pandemic times, presential training is not possible. Thus, a viable solution would be the use of laboratories based on virtual reality (VR).

Three-D scanning methods can be used to reconstruct a part for different industrial purposes, varying from reverse engineering (Guarato *et al.*, 2016, Olejnik *et al.*, 2018) to dimensional inspection of a gas turbine (Bösemann, 2016). A wide variety of scanners is available, classified as active or passive sensors. In the active sensors, as in laser scanning, energy is transmitted to the scene and the reflected energy is retrieved. In contrast, passive sensors do not transmit energy but use natural light available to acquire information (Bhatla *et al.*, 2020). An example of a technique that uses this last type of sensor is photogrammetry. Guerra *et al.* (2018) state that the advantages of passive systems in comparison with active ones are lower costs, are more compact and easier to use. In contrast, one hindrance is that they tend to be slower and less precise.

Laser scanners work based on the structure light scanning (SLS) principle, which applies light lines on the object and uses a camera to acquire patterns of deformation. Then, it calculates the coordinates x, y, and z through active triangulation (Keaveney *et al.*, 2016, Rodríguez *et al.*, 2017, Singhatham *et al.*, 2019).

By definition, photogrammetry is an optical measurement technique that is used to obtain the geometry, displacement, and deformation of a structure using photographs or digital images from different viewing angles (Taqriban *et al.*, 2019, Júnior *et al.*, 2009). It was initially developed for military aerial and terrestrial applications (Taqriban *et al.*, 2019), but it was later adapted for industry in the Close Range mode (Martín and Gonzalvez, 2018). It uses the alignment of reference

points of a large number of 2D images to triangulate the point cloud to form a 3D model (Bhatla *et al.*, 2020, Keaveney *et al.*, 2016, Waterhouse *et al.*, 2017, James *et al.*, 2017). This procedure is also known as Structure from Motion (SfM) (Kovynev and Zaslavsky, 2021).

Special attention should be given during image acquisition in terms of illumination, focus, and depth of field (Adami *et al.*, 2015). The component must have a texture (visual pattern, color) for the software to find the points of correspondence (Waterhouse *et al.*, 2017). Besides general inspection (Maccormick *et al.*, 2011), photogrammetry has been used in medicine (Taqriban *et al.*, 2019, Odeh *et al.*, 2019, Palousek *et al.*, 2014), biological sciences (Keaveney *et al.*, 2016), civil construction (Kovynev and Zaslavsky, 2021) and archeology (Gaboutchian *et al.*, 2020), with the last application is the most commonly found in the literature. It is worth mentioning the importance of this knowledge for the reconstruction of the Notre Dame Paris monument after the 2019 fire. Reconstruction was only possible because a company, specialized in 3D digitalization, had scanned the entire building between 2014 and 2016, using photogrammetry (Bock, 2019).

Although laser scanning systems are generally more accurate when compared to photogrammetry, they require a much higher investment, they are often not portable, require specific training (Bahtla *et al.*, 2020), and do not include texture (color) in the model (Adami *et al.*, 2015). A commercial laser scanner system costs around US$ 40,000, while photogrammetry system consisting in a DSLR camera and a treatment software, which can be an open-source one, may have a final cost around US$ 1,000.

Low cost and simplicity of operation are essential for photogrammetry diffusion in industries. The presence of texture (color) in the model is mandatory for the identification of some discontinuities. Photogrammetry models are named global models, since they present geometry and texture (color) (Martín and Gonzalvez, 2019). However, there are some AM inherent challenges that have not been investigated before. Most studies are focused on the inspection of geometrical characteristics and welding (Evans *et al.*, 2018). Waterhouse *et al.* (2017) stated that some AM parts do not present sufficient texture to apply the photogrammetry technique. In order to solve this problem, they proposed a laser speckle projection system. Reflectivity is also an issue (Guerra *et al.*, 2018). Despite the lack of information about the subject, recent publications demonstrate that both photogrammetry (Evans *et al.*, 2018, Bahnini *et al.*, 2020) and laser scanners (Xiong *et al.*, 2020) are already being used to inspect AM components. In none of the cases, a component manufactured by WAAM was analyzed.

Therefore, the following questions arise: is it possible to inspect metallic components manufactured by AM by using photogrammetry? Both scanners present a submillimeter accuracy, but is it sufficient in the case of WAAM? If positive, remote inspection becomes viable and will be of easy diffusion. This will bring not only benefits in terms of cost-saving, but also in accuracy improvement relative to the traditional gauge kits, digital recording, in which data can be used considering the concept of industry 4.0 and, finally, it will allow the development of virtual learning platforms.

2. METHODOLOGY

To confirm that the photogrammetry system is adequate for scanning and measuring parts produced by WAAM, the object selected for inspection (Figure 2), was manufactured through WAAM by using the MIG/MAG process and carbon steel wire (AWS ER70S-6), and it has its nominal dimensions of height, outer diameter, and inner diameter shown in Figure 2. This sample was selected because it presents typical dimensions of a component manufactured by WAAM and the main challenges regard the light reflection (metal) for image acquisition and surface waviness assessment.

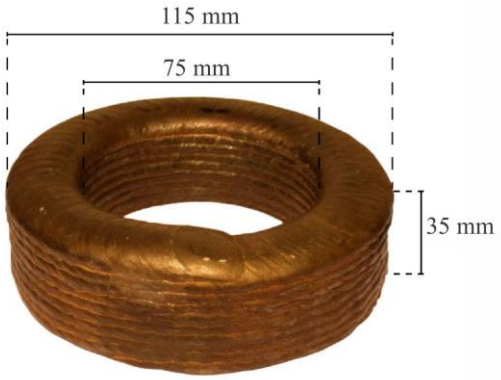

Figure 2. Sample manufactured through WAAM selected for inspection with nominal dimensions of 35 mm (height), 115 mm (outer diameter), and 75 mm (inner diameter).

In order to acquire the images for photogrammetry, a DSLR Nikon D5300 camera coupled with a NIKKOR 18-55 mm lens, mounted on a tripod for stabilization, was used. This camera is equipped with an Advanced Photo System type-C (APS-C) sensor that measures 23,4 x 15,6 mm.

Yet, picture luminosity can be affected by ISO parameter (what measures the camera's sensitivity to light), aperture, and shutter speed, so the greater the ISO, the wider the aperture, and the slower the shutter speed, the brighter the picture gets. Nevertheless, these three parameters also have other effects on the picture, besides increasing its luminosity. The greater the ISO, the less sharpness the picture has; the wider the aperture opening, the narrower is the depth of field; and the slower the shutter speed, the most likely the picture will have motion blur. It is important to point out that focal length directly restricts aperture, consequently, it also influences the depth of field and the amount of light that reaches the sensor. Therefore, after several tests, the following parameters were selected and fixed: focal distance 29 mm, aperture f/25, ISO 2500, and shutter speed 1/30 seconds.

Lighting was provided by two 1.4 W LED lamps, minimizing shadows on the object surface, since proper illumination is essential for optical systems (Riggio *et al.*, 2015). A turntable also was used, and the sample was placed at its center, similarly to Fregonese et al. (2019) and Porter et al. (2015). This allows greater efficacy on image acquisition, since the camera is stationary, while the object is rotated. Figure 3 presents the experimental setup for image acquisition.

Figure 3. Experimental setup for image acquisition.

Photograph distribution was defined as 24 images per 360° (15° interval between each image, such as James et al. [2017]) and 7 full rotations of the object, in a total of 168 images, changing the parameter “h” (height) and the focus between the outer and inner faces, with the camera pointing to the center of the object. This procedure leads to high image superposition since the object presents a similar texture pattern through most of its surface, which could easily be mistaken by the software used for image alignment and processing. Parameter “b” represents the horizontal distance between the center of the object and the center of the camera base, which was 250 mm for all measurements. Figure 4 illustrates the geometrical parameters “h” and “b”. In Table 1 “h” and focus, variation is shown as a function of rotation. This was necessary since it is not possible to focus the entire object, with the camera set to an aperture of F25. In order to deliver a sequence of images that cover all the object focused, it was necessary to vary these two parameters.

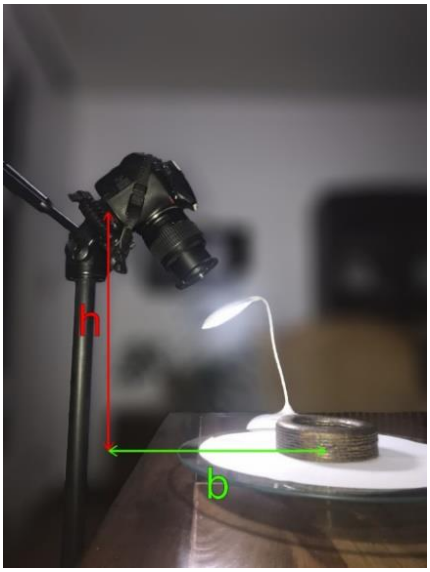

Figure 4. Camera positioning parameters. “h” stands for the vertical distance between the camera and the turntable and “b” stands for the horizontal distance between the base of the camera and the object center.

Table 1. Camera height and image focus as a function of the rotation number.

Rotation	Height “h” [mm]	Focus
1	270	Inner distal
2	240	Inner distal
3	210	Inner distal
4	180	Inner distal
5	180	Outer frontal
6	150	Outer frontal
7	120	Outer frontal

It is important to mention that rotations 4 and 5 were done at the same height, but with different focus, as indicated in Figure 5. This procedure helps image alignment since, even with lens aperture set at f/25 (second smallest aperture possible for the focal length, and lens used), it is not possible to keep the whole object focused on a single image due to its proximity to the camera.

Figure 5. Outer frontal and Inner distal focus.

All 168 acquired photographs were imported into the open-source software Meshroom, which was used to process and generate the 3D model. Other open-source software is also available (Griwodz *et al.*, 2021). The interface with the project and 3D model generated is shown in Figure 6 (a) and (b), respectively.

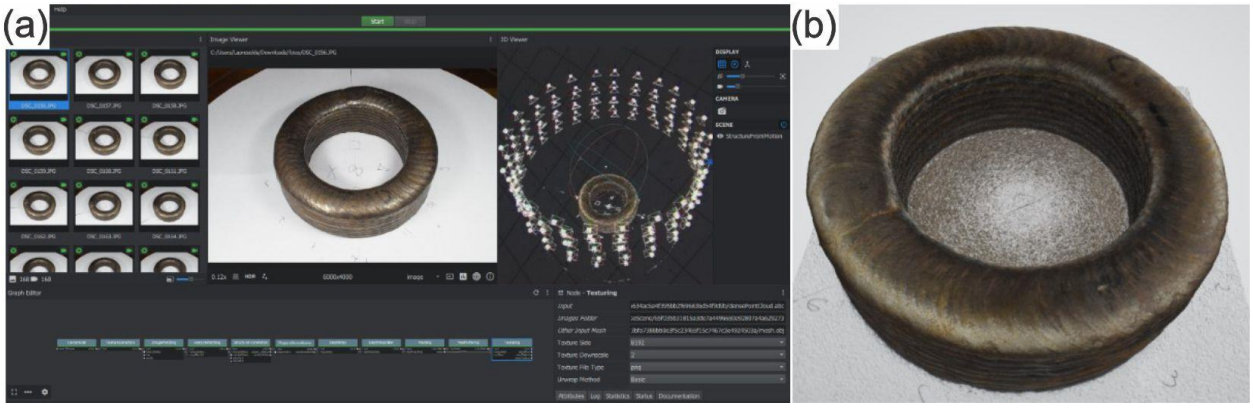

Figure 6. (a) Meshroom software interface. (b) The 3D generated model.

The reconstruction method involves 7 main steps (Griwodz *et al.*, 2021): Feature extraction, Image matching, Feature matching, Structure from Motion (SfM), Depth map estimation, Meshing, and Texturing. Feature extraction is the step in which distinctive points in every individual image are detected based on invariant properties such as, lighting, scale, and rotation. These points are then used to form the basis for finding the relative spatial position of the camera in each image. In order to find corresponding points among the images, in the Image matching step each pair of images are compared and matched. After that, each pair of image has their features matched (Feature matching step) allowing the future determination of a 3D structure from the 2D positions.

In turn, the Structure from Motion step consists in the creation of tracks (possibilities to represent a point in space, visible from multiple camera angles). The tracks are created from the fusion of the previous computed matches and are used to generate a sparse 3D representation. On the Depth map estimation step the software tries to estimate a depth value for every pixel. It is required that the area is visible by at least 2 camera angles that were validated by the SfM.

The last two steps taken by the software to create the 3D model are Meshing and Texturing. Meshing consists in the creation of a dense 3D mesh. For that, all depth maps are merged into one dense point cloud from which a surface is

extracted. The final step projects the best textures of each region (determined through the computation of the resolution of the triangle in all images seeing it) onto the mesh.

Still regarding the open-source software, there is a parameter on the Depth Map and Texture steps that has a high impact on the quality of the final 3D model generated, which is the downscale parameter. Since these steps require a high computational power, the software offers the option of downscaling the quality of the results of these steps. Therefore, if this parameter is set to 1, the software will operate at its highest capacity. If it is set to 8 or 16 the quality will drop proportionally but the processing time will be considerably reduced. As the processing time with the downscale set to 1 was unfeasible for this work we decided to operate with the downscale set to 2 on both steps, with which it was possible to generate the 3D model with a high quality under a reasonable time.

In order to determine the suitability of photogrammetry for inspection, a commercial laser scanning system CREAFORM Handy SCAN 307 was used to obtain the reference model. This equipment has two cameras, 7 crossed lasers, a scanning area of 275 per 200 mm, and it is able to make 480,000 measurements per second, with accuracy of 0.040 mm. The scanner must be calibrated with a standard provided by the manufacturer and the shutter must be adjusted for natural lighting, before scanning any object. Similarly to the photogrammetry process, a turntable is used. Required reference targets must be static in relation to the sample object and placed between 50 to 100 mm from each other. Figure 7 shows the experimental setup for laser scanning.

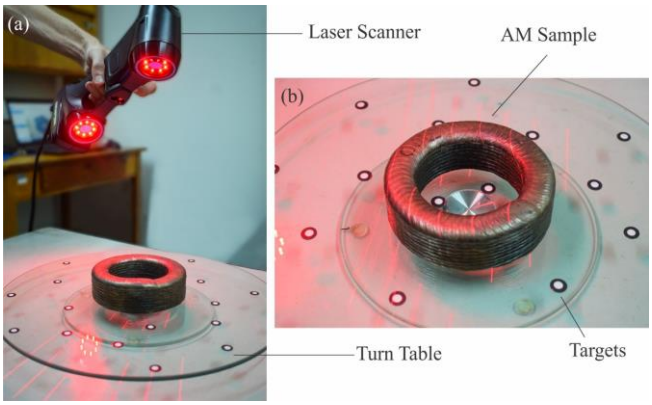

Figure 7. (a) Experimental setup for laser scanning. (b) Placement of targets.

The resultant model was built using VX Elements software, created during the scanning procedure (Figure 8).

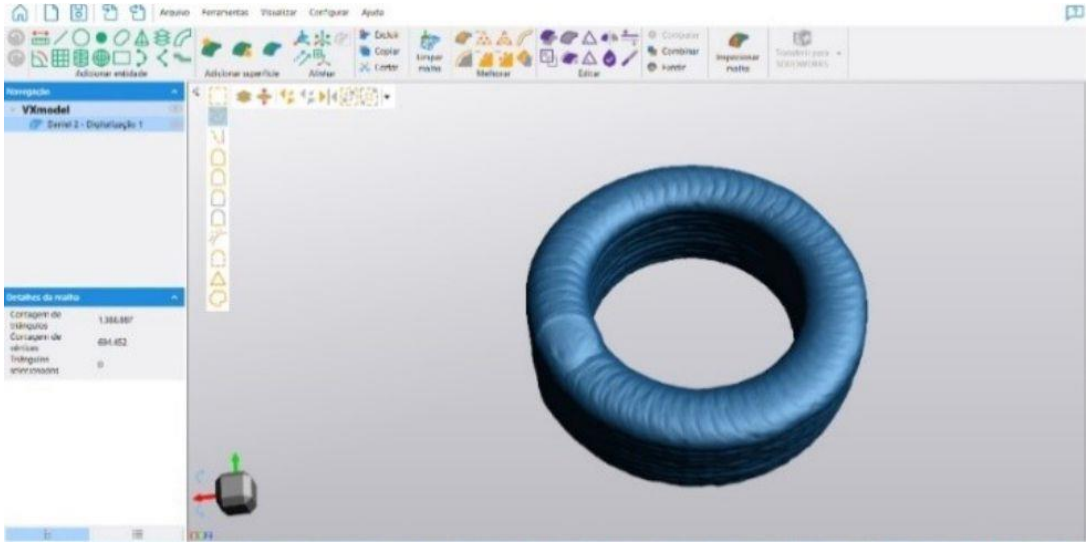

Figure 8. VX Elements software interface with the final model generated by the 3D laser scanner.

The open-source software CloudCompare was used for alignment and scale adjustment of the point clouds (one obtained with photogrammetry process and one obtained with the laser scanner sensor). A comparison of the distance between point clouds of the two measurement processes was made by calculating the minimum distance between each point of the models using the algorithm of the nearest neighbor, in the same software. Figure 9 shows the interface of CloudCompare software.

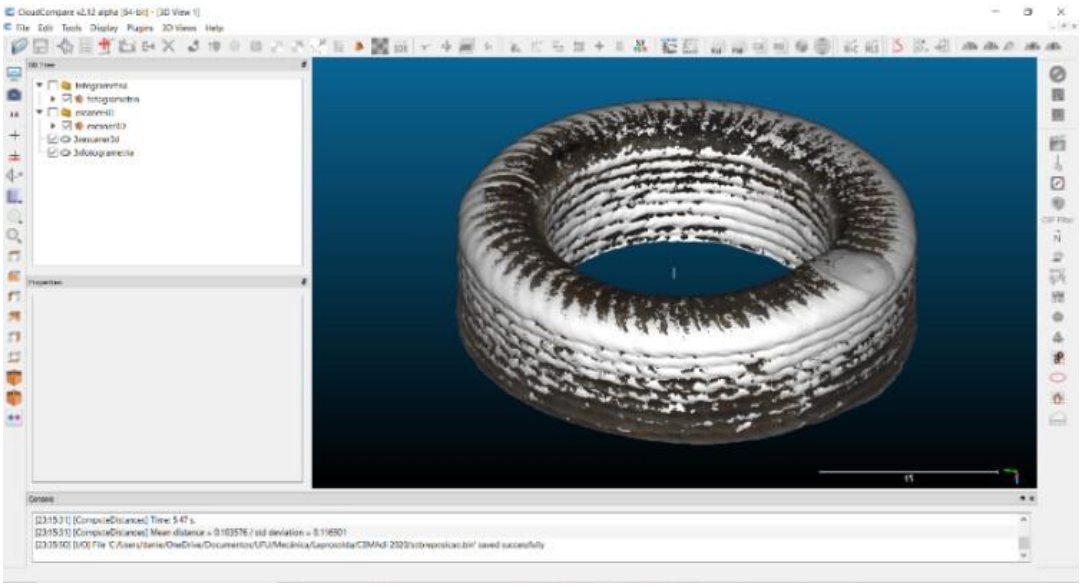

Figure 9. CloudCompare software interface with the aligned point clouds generated by the two measurement methods (photogrammetry and laser scanner).

Data processing for both photogrammetry and laser scanning data was done with the same computer with the following specifications: HP Compaq ZBook15 G3 with Intel® Core™ i7-6820HQ, Windows® 10 Pro 64bits, Nvidia Quadro M1000M 2 Gb.

3. RESULTS

Suitability of photogrammetry for inspection of the AM component was evaluated with CloudCompare open source software. Figure 10 presents the results of point cloud superposition considering photogrammetry and laser scanning methods.

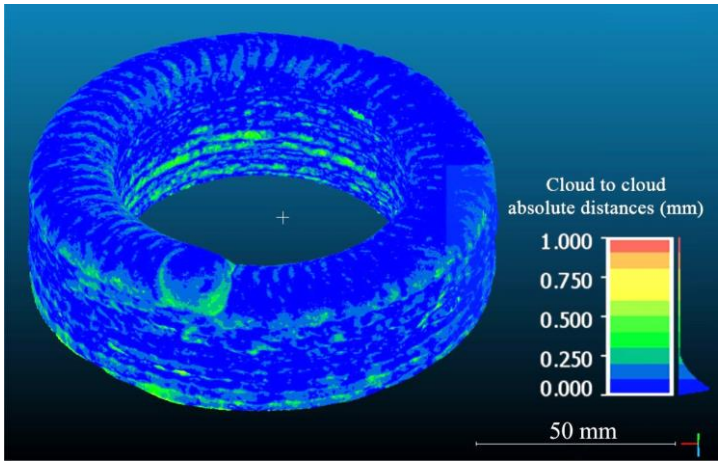

Figure 10. Point cloud superposition considering photogrammetry and laser scanning models.

The scale represents the divergence level. Since the majority of the regions are blue, the models match. Some points are green, which corresponds to a 0.500 mm deviation. A more detailed analysis was done with the cloud-to-cloud absolute distance histogram (Figure 11).

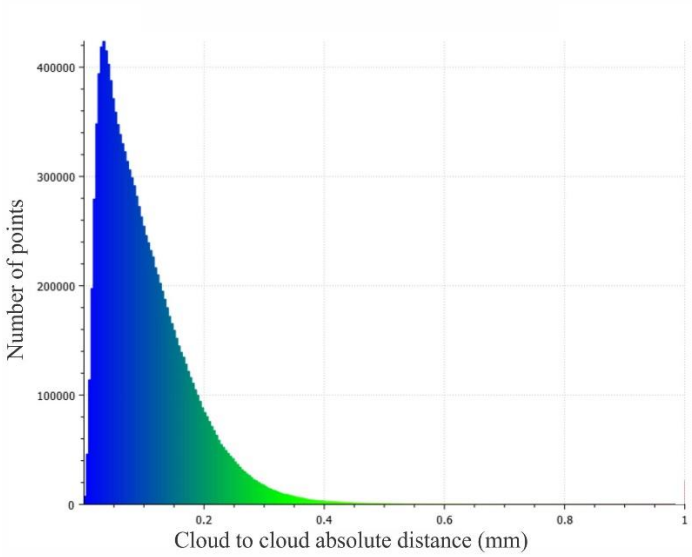

Figure 11. Cloud to cloud absolute deviation histogram considering photogrammetry and laser scanning models.

The point cloud generated by the photogrammetry process presented an average distance of 0.104 mm in relation to the point cloud of the reference model obtained with the laser scanner. Since the laser scanner has a 0.040 mm accuracy, photogrammetry estimated accuracy is 0.144 mm (0.104 ± 0.040 mm). As a metrological rule, the measuring instrument should be accurate to 1/10th of the tolerance. Therefore, in this case, photogrammetry is suitable for measurements with tolerance above 1.440 mm and the laser scanner, for measurements with tolerance above 0.400 mm.

This result is better than others found in the literature, such as those from Vacca (2019), who analyzed a 28 m diameter structure and obtained an average discrepancy of 0.03 m between photogrammetry and laser scanning techniques, i.e., there was a proportion of 1.07 x 10-3. In the present study, the object outer diameter has approximately 115 mm, and the average distance between the two models are 0.104 mm, i.e., a proportion of 9.04 x 10-4, which represents greater accuracy. Based on that, considering the dimension inspection of diameters, height, and width of the selected component, photogrammetry technique is suitable since its measures are far above 1.4 mm. The absence of texture color representation is not an issue here, differently from Waterhouse's et al. work (Waterhouse *et al.*, 2017), in addition, reflectivity is not a problem as well, although mentioned by Guerra *et al.* (2018).

A comparison between the analyzed systems (photogrammetry and laser scanning) is presented in Table 3.

Table 2. Comparison between photogrammetry and laser scanning

Photogrammetry		Laser scanning	
Camera setup time	5 min	Calibration time	10 min
Image acquisition time	15 min	Scanning time	15 min
Computer processing time	320 min	Computer Processing time	5 min
Total processing time	340 min	Total processing time	30 min
Number of points	13,279,883	Number of points	20,000,455
Accuracy	0.144 mm	Accuracy	0.040 mm
Texture	Yes	Texture	No
Color	Yes	Color	No
Measurement of typical dimensions	Yes	Measurement of typical dimensions	Yes
Measurement of waviness	No	Measurement of waviness	Yes
Qualitative 2D analysis of waviness	Yes	Qualitative 2D analysis of waviness	Yes
System cost	US$ 988	System cost	US$ 40,328

The laser scanning system has better processing time and it is more accurate than the photogrammetry one. However, for WAAM inspection purposes, the accuracy of photogrammetry is sufficient when the measured dimension is greater than 1.440 mm, which is true for the component diameter, for example. Color representation is fundamental for inspection and is possible only in photogrammetry, since some defects can be easily detected on the surface even if they may not exhibit large geometrical variations. Another important feature is the color pattern obtained by photogrammetry system. In the case of setback with slag (silicon islands) entrapment between layers, the photogrammetry system could provide visual identification of critical spots by the yellowish color identification. Finally, the main advantage of photogrammetry is its reduced cost, which corresponds to 2.4% of the laser scanning cost and can contribute to the diffusion of

photogrammetry 3D scanning technology in industries. Moreover, images can be acquired in loco by one person and post treatments can be done by another person that are not necessarily near the inspected part, which is another great advantage of this inspection method.

Since the photogrammetry methodology presented a sufficient accuracy for WAAM, remote inspection becomes viable. This will benefit the industry cost-wise, and in accuracy improvement relative to the traditional inspection methods, in which data can be used considering the concept of industry 4.0 and, finally, it will allow the development of virtual learning platforms. A practical way of performing the remote inspection is shown in Figure 12. It is a low-cost VR glass coupled to a mobile phone. The 3D model of the subject, saved in .obj format, can be sent to the mobile phone and visualized using the 3D Model Viewer App.

Figure 12. VR glass coupled to a mobile phone with the 3D Model Viewer app to execute remote inspection.

4. CONCLUSION

The photogrammetry 3D scanning technique is viable for the inspection of AM metallic components with dimensions above 1.440 mm. Although laser scanning is faster in terms of total processing time, the accuracy of 0.144 mm (0.104 ± 0.040 mm) observed with photogrammetry is adequate for the inspection of the main geometrical characteristics, such as part diameter.

The photogrammetry system is a low-cost solution (only 2.4% of the laser system cost) and it generates models with texture and color, which are not possible in the laser scanning system. Texture is fundamental for visual inspection, as discontinuities that do not show large geometrical variations can be identified on the surface. Photogrammetry reduced cost is due to the simplicity of the system, consisting of a DSLR camera and open-source software.

Therefore, the proposed remote inspection system is viable and easy to implement and replicate. This brings benefits in terms of cost-saving, increased inspection accuracy in comparison to traditional gauge kits, it provides digital recording of results, and its data can be used considering the concept of Industry 4.0, and finally it allows the development of virtual learning platforms.

5. ACKNOWLEDGEMENTS

The authors would like to thank the technical and financial support provided by Petrobras, ANP, CAPES, CNPq, and FAPEMIG.

6. REFERENCES

Adami, A., Balletti, C., Fassi, F., Fregonese, L., Guerra, F., Taffurelli, L. and Vernier, P., 2015. The bust of Francesco II Gonzaga: from digital documentation to 3D printing. ISPRS Annals of the Photogrammetry, Remote Sensing and Spatial Information Sicences. doi: 10.5194/isprsannals-II-5-W3-9-2015.

Bacciaglia A., Ceruti A., Liverani A., 2020. Photogrammetry and additive manufacturing based methodology for decentralized spare part production in automotive industry. Proceedings of the 3rd International Conference on Intelligent Human Systems Integration (IHSI). doi: 10.1007/978-3-030-39512-4_121.

Bahnini I., Zaman U.K., Rivette M., Bonnet N., Siadat A., 2020. Computer-aided design (CAD) compensation through modeling of shrinkage in additively manufactured parts. Int J Adv Manuf Technol 106:3999–4009. doi: 10.1007/s00170-020-04924-8.

Bai J.Y., Yang C.L., Lin S.B., Dong B.L., Fan C.L., 2016. Mechanical properties of 2219-Al components produced by additive manufacturing with TIG. Int J Adv Manuf Technol 86:479–485. doi: 10.1007/s00170-015-8168-x.

Bhatla A., Choe S.Y., Fierro O., Leite F., 2020. Evaluation of accuracy of as-built 3D modeling from photos taken by handheld digital cameras. Autom Constr 28:116–127. doi: 10.1016/j.autcon.2012.06.003.

Bock P., 2019. How Notre Dame is being rebuilt from 50 billion scraps of data. https://www.wired.co.uk/article/notre-dame. Accessed 30 June 2021.

Bösemann W., 2016. Industrial photogrammetry - accepted metrology tool or exotic niche. The International Archives of the Photogrammetry, Remote Sensing and Spatial Information Sciences XLI-B5:15-24. doi: 10.5194/isprsarchives-XLI-B5-15-2016.

Chua Z.Y., Ahn I.H., Moon S.K., 2017. Process Monitoring and Inspection Systems in Metal Additive Manufacturing : Status and Applications. International Journal of Precision Engineering and Manufacturing-Green Technology 4:235–245. doi: 10.1007/s40684-017-0029-7.

Dos Santos L.C.P., Malheiros F.C., Guarato A.Z., 2019. Surface parameters of as-built additive manufactured metal for intraosseous dental implants. J Prosthet Dent 0(0). doi:10.1016/j.prosdent.2019.09.010

Evans S., Jones E., Fox P., Sutcliffe C., 2018. Photogrammetric analysis of additive manufactured metallic open cell porous structures. Rapid Prototyping Journal 8:1380–1391. doi: 10.1108/RPJ-05-2017-0082.

Fregonese L., Giordani N., Adami A., Bachinsky G., Taffurelli, Rosignoli O., Helder J., 2019. Physical and virtual reconstruction for an intergrated archaeological model: 3D print and maquete. The International Archives of the Photogrammetry, Remote Sensing and Spatial Information Sciences XLII-2/W15: 481-487. doi:10.5194/isprs-archives-XLII-2-W15-481-2019.

Gaboutchian A.V., Knyaz V.A., Leybova N.A., Simonyan H.Y., Novikov M.M., Apresyan S.V., Cherebylo S.A., Petrosyan G.R., 2020. 3D Reconstruction and image processing of anthropological archaeological findings. The International Archives of the Photogrammetry, Remote Sensing and Spatial Information Sciences XLIII-B2:845–850. doi: https://doi.org/10.5194/isprs-archives-XLIII-B2-2020-845-2020.

Griwodz C., Gasparini S., Calvet L., Gurdjos P., Castan F., Maujean B., ... & Lanthony Y., 2021. AliceVision Meshroom: An open-source 3D reconstruction pipeline. In Proceedings of the 12th ACM Multimedia Systems Conference (pp. 241-247). https://doi.org/10.1145/3458305.3478443

Guarato A.Z., Loja A.C., Pereira L.P., Braga S.L., Trevilato T.R.B., 2016. Qualification of a 3D structured light sensor for a reverse engineering application. Optics and Measurement International Conference 10151:1–9. doi: 10.1117/12.2257601.

Guerra M.G., Volpone C., Galantucci L.M., Percoco G., 2018. Photogrammetric measurements of 3D printed micro fluidic devices. Additive Manufacturing 21:53–62. doi: 10.1016/j.addma.2018.02.013.

Hodonou C, Balazinski M, Brochu M, Mascle C (2019) Material-design-process selection methodology for aircraft structural components : application to additive vs subtractive. Int J Adv Manuf Technol 103:1509–1517. doi:10.1007/s00170-019-03613-5.

James D.W., Belblidia F., Eckermann J.E., Sienz J., 2017. An innovative photogrammetry color segmentation based technique as an alternative approach to 3D scanning for reverse engineering design. Computer Aided Design & Applications 14:1–16. doi: 10.1080/16864360.2016.1199751.

Jr A.A.G., Hofmann A.C., Fantin A.V., Santos J.M.C., 2009. Development and application of a pipelines. SPIE Europe Optical Metrology 7389:1-12 doi: 10.1117/12.827544.

Keaveney S., Gutierrez-heredia L., Keogh C., Reynaud E.G., 2016. Applications for advanced 3D imaging , modelling , and printing techniques for the biological sciences. 22nd Int Conf Virtual Syst Multimed 1–8. doi: 10.1109/VSMM.2016.7863157.

Kovynev M., Zaslavsky M., 2021. Review of photogrammetry techniques for 3D scanning tasks of buildings. Proceedings of the 28th Conference of Fruct Association. https://fruct.org/publications/acm28/files/Kov.pdf. Accessed 30 June 2021.

Li L, Zhang X., Cui W., Liou F., Deng W., Li W., 2020. Temperature and residual stress distribution of FGM parts by DED process : modeling and experimental validation. Int J Adv Manuf Technol 109:451–462. doi: 10.1007/s00170-020-05673-4.

Maccormick M., Hall A., Trower A., 2011. Component inspection and repair using 3D modelling photogrammetry technology. SPE Offshore Europe Oil and Gas Conference and Exhibition. doi: 10.2118/145513-MS.

Martín MR, Gonzalvez PR (2018) Learning based on 3D photogrammetry models to evaluate the competences in visual testing of welds. IEEE Global Engineering Education Conference (EDUCON) 1576–1581. doi: 10.1109/EDUCON.2018.8363422.

Martín M.R., Gonzálvez P.R., 2019. Learning methodology based on weld virtual models in the mechanical engineering classroom. Comp. Appl. Eng. Edu. 27:1113-1125. doi: 10.1002/cae.22140.

Neto F.C., Pereira M., Paes L.E.S., Fredel M.C., Bossa L.F., 2021. Effect of power modulation frequency on porosity formation in laser welding of SAE 1020 steels. Int J Adv Manuf Technol 112:2509-2517.

Odeh M., Levin D., Inziello J., Fenoglietto F.L., Mathur M., Hermsen J., Stubbs J., Ripley B., 2019. Methods for verification of 3D printed anatomic model accuracy using cardiac models as an example. Printing in medicine 5:1-12. doi:10.1186/s41205-019-0043-1.

Olejnik A., Kiszkowiak L., Dziubinski A., 2018. Aerodynamic modeling process using reverse engineering and computational fluid dynamics. Earth and Space 944-956.

Paes L.E.S., Ferreira H.S., Pereira M., Xavier F.A., Weingaertner W.L., Vilarinho L., 2021. Modeling layer geometry in directed energy deposition with laser for additive manufacturing. Surface & Coatings Technology 409:1-9 doi: 10.1016/j.surfcoat.2021.126897.

Paes L.E.S., Pereira M., Pereira A.S.P., Bórhoquez C.E.N., Weingaertner W.L., 2019. Power and welding speed influence on bead quality for overlapped joint laser welding. J Laser Appl 31: 022403-1-5 doi: 10.2351/1.5096110.

Paes LES, Pereira M, Weingaertner WL, Scotti A, Souza T (2019) Comparison of methods to correlate input parameters with depth of penetration in LASER welding. Int J Adv Manuf Technol 101:1157–1169. doi: 10.1007/s00170-018-3018-2.

Palousek D., Rosicky F., Koutny D., Stoklásek, Navrat .T., 2014. Pilot study of the wrist orthosis design process. Rapid Prototyping Journal 20:27–32. doi: 10.1108/RPJ-03-2012-0027.

Petrobras, 2019. Instalamos primeira peça de aço impressa em 3D em área operacional. https://nossaenergia.petrobras.com.br/pt/energia/instalamos-primeira-peca-de-aco-impressa-em-3d-em-area-operacional/#:~:text=Pesquisadores%20do%20Cenpes%2C%20Centro%20de,do%20original%20em%20ferro%20fundido. Accessed 30 June 2021.

Porter S.T., Roussel M., Soressi M., 2015. A simple photogrammetry rig for the reliable creation of 3D artifact models in the field lithic examples from the early upper paleolithic. Advances in Archaeological Practice 4:71–86. doi: 10.7183/2326-3768.4.1.71.

Riggio M., Sandak J., Franke S., 2015. Application of imaging techniques for detection of defects, damage and decay in timber structures on-site. Constr Build Mater 101:1241–1252. doi: 10.1016/j.conbuildmat.2015.06.065.

Rodríguez M.M., Gonzálvez P.R., Aguilera D.G., 2017. Feasibility study of a structured light system applied to welding inspection based on machine data. IEEE Sensors Journal 17:4217–4224.

Sartori F., Silva R.H.G., Dutra J.C., Paes L.E.S., Schwedersky M.B., Marques C., 2017. A comparative analysis of different versions if the MIG/MAG process modern variants for the root pass in orbital welding. Soldag e Insp 22:442–452. doi: 10.1590/0104-9224/SI2204.04.

Silva R.H.G., Paes L.E.S., Barbosa R.C., Sartori F., Schwedersky M.B., 2018. Assessing the effects of solid wire electrode extension (Stick out) increase in MIG/MAG welding. J Brazilian Soc Mech Sci Eng. 40:1-7 doi: 10.1007/s40430-017-0948-9.

Silva R.H.G., Paes L.E.S., Marques C., Riffel K.C., Schwedersky M.B., 2019. Performing higher speeds with dynamic feeding gas tungsten arc welding (GTAW) for pipeline applications. J Brazilian Soc Mech Sci Eng. 41:1-6 doi: 10.1007/s40430-018-1529-2.

Silva R.H.G., Paes L.E.S., Sousa G.L., Marques C., Viviani A.B., Schwedersky M.B., Pinto T.H.F.C., 2019. Design of a wire measurement system for dynamic feeding TIG welding using instantaneous angular speed. Int J Adv Manuf Technol 101:1651–1660. doi: 10.1007/s00170-018-3026-2.

Singhatham P., Srigate S., Tanachutiwat S., 2019. Designing of welding defect samples for data mining in defect detection and classification using 3D geometric scanners. Research Invention and Innovation Congress 1-6. doi: 10.1109/RI2C48728.2019.8999939.

Sohaib A., Amano K., Xiao K., Yates J.M., Whitfor C., Wuerger S., 2018. Colour quality of facial prostheses in additive manufacturing. Int J Adv Manuf Technol 96:881–894. doi: 10.1007/s00170-017-1480-x.

Taqriban R.B., Ariyanto M., Putra A.F.Y.S., Ismail R., 2019. 3D model of photogrammetry technique for transtibial prosthetic socket design development. International Seminar on Research of Information Technology and Intelligent Systems (ISRITI). doi: 10.1109/ISRITI48646.2019.9034670.

Truppel G.H., Angerhausen M., Pipinikas A., Paes L.E.S., 2019. Stability analysis of the Cold Metal Transfer (CMT) brazing process for galvanized steel plates with ZnAl4 filler metal. Int J Adv Manuf Technol 103:2485–2494. doi: 10.1007/s00170-019-03702-5.

Vacca G., 2019. Overview of open software for close range photogrammetry. The International Archives of the Photogrammetry, Remote Sensing and Spatial Information Sciences XLII-4/W14:26–30. doi:10.5194/isprs-archives-XLII-4-W14-239-2019.

Waterhouse D.S., Bointon P., Piano S., Leach R.K., 2017. Experimental comparison of photogrammetry for additive manufactured parts with and without laser speckle projection. Optical Measurement Systems for Industrial Inspection X. doi: 10.1117/12.2269507.

Xiong Y., Dharmawan A.G., Tang Y., Foong S., Soh G.S., Rosen D.W., 2020. A knowledge-based process planning framework for wire arc additive manufacturing. Adv Eng Informatics 45:101135. doi: 10.1016/j.aei.2020.101135.

7. RESPONSIBILITY NOTICE

The authors are the only responsible for the printed material included in this paper.